



ELSEVIER

Available online at www.sciencedirect.com

SCIENCE @ DIRECT®

Earth and Planetary Science Letters 214 (2003) 11–25

EPSL

www.elsevier.com/locate/epsl

Fossil ^{26}Al and ^{53}Mn in the Asuka 881394 eucrite: evidence of the earliest crust on asteroid 4 Vesta

L.E. Nyquist^{a,*}, Y. Reese^b, H. Wiesmann^b, C.-Y. Shih^b, H. Takeda^c

^a SRINASA Johnson Space Center, 2101 NASA Road 1, Houston, TX 77058, USA

^b MC-23, Lockheed-Martin Space Mission Systems and Service Co., 2400 NASA Road 1, Houston, TX 77058, USA

^c Research Institute, Chiba Inst. Tech., 2-17-1 Tsudanuma, Narashino City, Chiba 275-0016, Japan

Received 28 January 2003; received in revised form 17 June 2003; accepted 2 July 2003

Abstract

Asuka 881394 is a unique magnesian eucrite with pyroxenes that are Mg-rich like those of cumulate eucrites, but with a granulitic texture unlike the textures of cumulate eucrites. Plagioclase compositions are $\sim\text{An}_{98}$, and are even more calcic than those in cumulate eucrites. Pyroxene does not show pigeonite-to-orthopyroxene inversion textures, suggesting different crystallization conditions than those of cumulate eucrites. Mn–Cr isotopic analyses determined initial $^{53}\text{Mn}/^{55}\text{Mn} = (4.6 \pm 1.7) \times 10^{-6}$ and initial $\epsilon^{53}\text{Cr}_I = 0.25 \pm 0.17$ in A881394. This initial ^{53}Mn abundance corresponds to a formation interval $\Delta t_{\text{LEW}} = -6 \pm 2$ Ma relative to the LEW86010 angrite, implying an ‘absolute’ age of 4564 ± 2 Ma. Both the initial ^{53}Mn abundance and the initial $\epsilon^{53}\text{Cr}_I$ value for A881394 are identical to those previously determined for the HED parent body at the time of its differentiation. Al–Mg isotopic analyses determined initial $^{26}\text{Al}/^{27}\text{Al} = (1.18 \pm 0.14) \times 10^{-6}$, from which a formation interval $\Delta t_{\text{CAI}} = 3.95 \pm 0.13$ Ma is calculated relative to the canonical value $^{26}\text{Al}/^{27}\text{Al} = 5 \times 10^{-5}$ for CAI. Combining this formation interval with a recently reported Pb–Pb age of 4567.2 ± 0.6 Ma for CAI gives 4563.2 ± 0.6 Ma as the age of A881394, in excellent agreement with the age based on the Mn–Cr formation interval. Alternatively, the ^{53}Mn and ^{26}Al formation intervals of A881394 allow the Mn–Cr and Al–Mg timescales to be intercalibrated, suggesting that an ‘absolute’ CAI age of 4568 Ma is most consistent with the 4558 Ma Pb–Pb age of LEW86010. The initial ^{26}Al abundance existing in A881394 would have been insufficient to cause global melting in the HED parent body (probably asteroid 4 Vesta). Nevertheless, it could have been derived by radioactive decay over only ~ 2 Ma from an abundance that would have been sufficient to cause global melting. The higher value of molar $\text{Mg}/(\text{Mg}+\text{Fe}) = 0.57$ for A881394 than those of the ordinary (basaltic) eucrites ($\text{Mg}/(\text{Mg}+\text{Fe}) = 0.30\text{--}0.42$) suggests additional factors may have been important for magma genesis on the parent body. If ^{26}Al were the only heat source, partial melting would have been the major process in the interior of the parent body, and $\text{Mg}/(\text{Mg}+\text{Fe})$ would be lower in the melts than in the primordial source material. Late-stage accretion could have supplied relatively magnesian primordial material to the surface of the parent body, thereby increasing $\text{Mg}/(\text{Mg}+\text{Fe})$ in a shallow magma ocean from which A881394 crystallized, and also may have augmented ^{26}Al heating. The granulitic texture of A881394 may have been produced during residence in the thin, earliest, crust, kept hot by the magma beneath it. If ^{26}Al was, nevertheless, the *major* heat source for asteroidal melting, it may account for declining post-accretion heating of main belt asteroids with increasing heliocentric distance.

* Corresponding author. Tel.: +1-281-483-5038; Fax: +1-281-483-1573.

E-mail address: laurence.e.nyquist1@jsc.nasa.gov (L.E. Nyquist).

© 2003 Elsevier B.V. All rights reserved.

Keywords: eucrites; chronology; ^{26}Al heating; ^{26}Al timescale; ^{53}Mn timescale

1. Introduction

Antarctic meteorite Asuka 881394 (hereafter A881394) is a coarse-grained igneous rock composed of nearly equal amounts of mm-sized plagioclase and pyroxene crystals, and minor amounts of other minerals. The isotopic composition of its oxygen shows that this meteorite belongs to the howardite–eucrite–diogenite (HED) meteorite clan [1]. These meteorites are widely believed to come from the asteroid 4 Vesta, often characterized as the smallest terrestrial planet. Although A881394 is a eucrite, it is unlike other basaltic eucrites, because it contains magnesian pigeonitic pyroxene and very calcic feldspar. Normally, Mg-rich eucrites, i.e. cumulate eucrites, contain orthopyroxenes transformed from pigeonite by very slow cooling, like plutonic rocks in layered intrusions on earth. This eucrite shows a metamorphic, granulitic, texture unlike the adcumulate texture of the better-known cumulate eucrites. Plagioclase compositions in A881394 are An_{98} , and are even more calcic than those in lunar highland rocks. Its old Al–Mg and Mn–Cr ages and unique mineralogical features are clear evidence that this rock is the oldest basalt yet recovered from the HED parent body, and a portion of the oldest planetary crust known to exist anywhere in the solar system.

2. Mineralogy–petrology of A881394

A polished thin section of A881394,52-2 supplied from the National Institute of Polar Research (Tokyo, Japan) has been employed for mineralogical and petrographic studies. Elemental distribution maps of Si, Mg, Al, and Cr were obtained by electron probe microanalysis (EPMA) at the Ocean Research Institute of the University of Tokyo. Modal abundances (vol%) of minerals derived from these maps are: pyroxene 49.3%, plagioclase 44.9%, silica mineral 5.3%,

and chromite 0.5%. Fig. 1 shows plane- and cross-polarized views of a thin section of the meteorite. Pale brown pyroxene crystals 0.4–1.5 mm in size are connected to form a granular texture. EPMA of exsolved augite lamellae, $\text{Ca}_{42}\text{Mg}_{39}\text{Fe}_{19}$, shows they are well separated in chemical composition

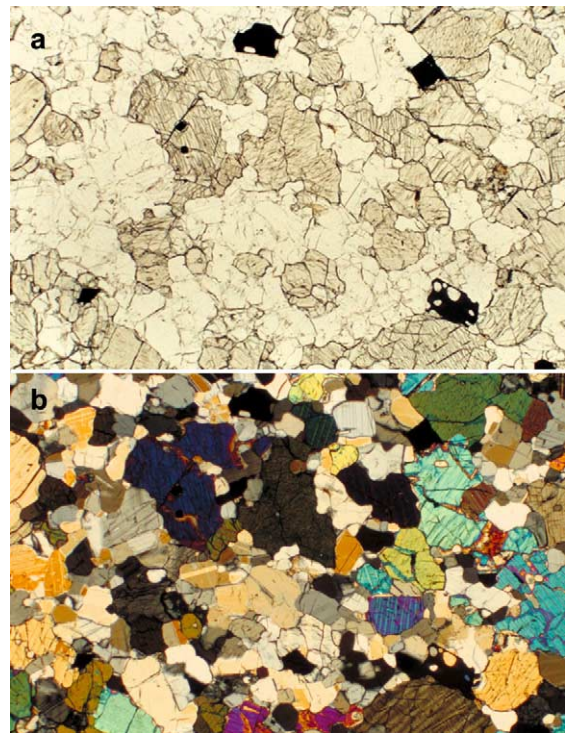


Fig. 1. (a) Plane-polarized view of Asuka 881394. The width is 5.0 mm. The coarse-grained, granulitic texture of pyroxene (tan) and plagioclase (off-white) is clearly visible. A large chromite grain at the lower right (black) poikilitically encloses plagioclase. (b) Same view as (a), but in cross-polarized light. Note pronounced exsolution lamellae in the pyroxene grain (dark blue) towards the upper left from the large chromite grain. A large plagioclase region, off-white and more visible in (a), extends from the central region towards the bottom of the photograph, and is seen in cross-polarized light to be composed of many smaller crystals. To the right and below the chromite is another pyroxene grain (yellow), and to its lower right is an irregularly shaped grain of silica (black).

Table 1
Chemical compositions (wt%) of minerals in A881394 eucrite

Minerals	Plagioclase	Silica	Chromite Small xls ^a	Pigeonite Bulk ^b	Augite Lamellae	Low-Ca Px Host
No. Meas.	26	8	42	169	7	7
SiO ₂	43.94	100.08	0.02	52.02	52.24	51.81
TiO ₂	0.01	0.11	3.87	0.27	0.45	0.22
Al ₂ O ₃	35.46	0.11	9.10	0.65	1.34	0.48
FeO	0.19	0.09	32.45	23.12	11.02	26.66
MnO	0.01	0.02	0.54	0.80	0.47	0.88
MgO	0.09	0.00	2.14	17.11	13.44	18.11
CaO	20.05	0.04	0.05	5.23	20.51	0.83
Na ₂ O	0.22	0.02	0.01	0.01	0.02	0.01
K ₂ O	0.01	0.01	0.00	0.01	0.01	0.01
Cr ₂ O ₃	0.02	0.00	51.31	0.52	0.85	0.42
V ₂ O ₃	0.01	0.00	0.53	0.02	0.04	0.02
Total	99.99	100.48	100.02	99.76	100.39	99.44

^a Average of several small crystals.

^b Average of line analyses across the exsolved lamellae.

from host low-Ca pyroxene, Ca₂Mg₅₄Fe₄₄ (Table 1). The bulk pyroxene composition obtained by line analyses with the EPMA is Ca₁₃Mg₅₀Fe₃₇. The widths of augite lamellae reach up to 10 μm. The host pigeonite does not show inversion textures indicating transformation from pigeonite to orthopyroxene, suggesting that the cooling history of A881394 differs from that of cumulate eucrites. Plagioclase regions up to 2 mm in longest dimension (off-white in Fig. 1a) fill the interstices between grains, and are composed of rounded, smaller crystals typically ~0.1–0.4 mm in diameter, as shown in the cross-polarized view (Fig. 1b). Plagioclase grains occasionally reach sizes of ~0.5 × 1.0 mm. Grains of a silica mineral up to 0.9 mm in length are distributed among plagioclase and pyroxene. This texture is unique among eucrites, and is different from those of recrystallized eucrites such as A881388. A large (0.55 × 0.30 mm) chromite grain at the lower right in Fig. 1 poikilitically encloses plagioclase, evidence of thermal metamorphism.

3. Mn–Cr formation interval

Conventional Rb–Sr and Sm–Nd ages of A881394 are ~4.4–4.5 Ga (1 Ga = 10⁹ yr). Also, excess ¹⁴²Nd in A881394 corresponds to an initial

abundance of the parent nuclide, ¹⁴⁶Sm, of ¹⁴⁶Sm/¹⁴⁴Sm = 0.0074 ± 0.0012 [2], nearly identical to ¹⁴⁶Sm/¹⁴⁴Sm = 0.0076 ± 0.0009 in the LEW86010 angrite [3]. Thus, newly synthesized ¹⁴⁶Sm, which has a half-life (*t*_{1/2}) for radioactive decay of 103 Ma (1 Ma = 10⁶ yr), was present in the rock when it crystallized. The ¹⁴⁶Sm–¹⁴²Nd formation interval of A881394 relative to LEW86010, Δ*t*_{LEW}, is 4 ± 26 Ma, confirming an ancient age. These observations prompted a search for evidence of shorter-lived ⁵³Mn (*t*_{1/2} = 3.7 Ma) and ²⁶Al (*t*_{1/2} = 0.73 Ma) in A881394.

Cr isotopic analysis followed the procedures of [3]. Table 2 presents the Mn–Cr isotopic data for A881394 and three other Asuka eucrites that were analyzed concurrently with it: A87272, A881388, and A881467. Values of ε(⁵³Cr) ~ 1.0 in the eucrites show that ⁵³Cr is enriched relative to that in the terrestrial standard by about 1 part in 10000. For A881388 and A87272, there are no apparent correlations between ε(⁵³Cr) and ⁵³Mn/⁵²Cr for data for different mineral separates (Fig. 2). The lack of variation of ε(⁵³Cr) among the mineral phases of these meteorites shows that either all the ⁵³Mn had decayed before the meteorites crystallized from a magma, or that the Cr isotopic composition was homogenized among the mineral phases after crystallization. In contrast, the low ε(⁵³Cr) value for A881394 chromite, correspond-

Table 2
Mn–Cr analytical results for Asuka eucrites A881394, A87272, A881388, and A881467

Sample ^a	Weight (mg)	Mn ^b (ppm)	Cr ^b (ppm)	⁵⁵ Mn/ ⁵² Cr ^c	$\epsilon(^{53}\text{Cr})^d$
(1) Eucrite A881394					
WR	5.1	3196	2442	1.48 ± 0.08	0.79 ± 0.30
Px	13.1	5830	3878	1.70 ± 0.09	0.97 ± 0.20
Chr	2.2	3634	317100	0.013 ± 0.001	0.26 ± 0.17
(2) Eucrite A87272					
WR	9.2	4231	1642	2.91 ± 0.15	1.07 ± 0.27
Chr	0.1	860	22220	0.044 ± 0.002	1.28 ± 0.20
Px	9.9	7013	1744	4.54 ± 0.23	0.99 ± 0.20
Silicates	25.17	6042	4483	1.52 ± 0.08	0.85 ± 0.18 0.74 ± 0.26
(3) Eucrite A881388					
WR	6.1	5538	2120	2.95 ± 0.15	1.11 ± 0.26
Chr	0.1	2030	6020	0.05 ± 0.02	1.17 ± 0.21
Px	6.5	7886	948	9.40 ± 0.47	0.89 ± 0.26
(4) Eucrite A881467					
WR	6.35	5435	1829	3.36 ± 0.17	1.07 ± 0.27
Chr	0.53	4381	249200	0.02 ± 0.001	0.87 ± 0.28
Opq(l)	7.19	4434	10684	0.47 ± 0.024	1.04 ± 0.35
Px	7.35	3917	492	8.99 ± 0.45	1.40 ± 0.26

^a WR = whole rock, Px = pyroxene, Chr = chromite, Opq-(l) = opaques leachate.

^b Determined by graphite furnace atomic absorption analysis (GFAA, analyst: C. Galindo of Hernandez Eng.) and inductively coupled plasma-source mass spectrometry (ICP-MS, analyst: C.M. Kuo of Wyle Labs).

^c Error limits are ± 5%.

^d $\epsilon(^{53}\text{Cr}) = 10000 \times [(^{53}\text{Cr}/^{52}\text{Cr})_{\text{sample}} / ((^{53}\text{Cr}/^{52}\text{Cr})_{\text{standard}} - 1)]$.

$(^{53}\text{Cr}/^{52}\text{Cr})_{\text{standard}} = 0.1134576 \pm 46$ for 19 runs of the JSC terrestrial standard normalized to $^{50}\text{Cr}/^{52}\text{Cr} = 0.0518585$ [5]. The error limit for the standard analyses is $\pm 2\sigma_p$ and corresponds to the last figures. The error limits for the samples are the greater of $\pm 2\sigma_m$ of the sample runs, or $\pm 2\sigma_m$ for an equal number of standard runs. σ_p = standard deviation of the population; σ_m = standard deviation of the mean.

ing to low ⁵⁵Mn/⁵²Cr, shows that chromite in this meteorite formed prior to complete decay of ⁵³Mn, and that the Cr isotopic composition was not subsequently equilibrated among mineral phases.

The lower Mn concentration and the higher Cr concentration in the bulk sample of A881394 than for bulk samples of the other three eucrites results in a ⁵⁵Mn/⁵²Cr ratio in A881394 that is only about half that in the others. Consequently, the Cr isotopic composition in A881394 is relatively non-radiogenic compared to that in the other eu-

crites. A881394 is a coarse-grained sample for which sampling heterogeneity is likely to be a factor for the ~5 mg bulk sample. Bulk samples of the eucrites were taken from larger (0.6–2.1 g) samples which had been crushed to <150 μm grain size, but without special precautions to make them representative of the larger samples. ‘Bulk’ means only that these samples are unseparated. The NIPR value of ⁵⁵Mn/⁵²Cr = 1.12 for A881394 [4] is ~25% lower than our value of 1.48, in agreement with the observation that A881394 has an unusually low Mn/Cr ratio. Our average ⁵⁵Mn/⁵²Cr = 3.07 for the other three eucrites is 8% higher than the average (2.83) of the NIPR published values [4]. The improved agreement for the other eucrites is probably a consequence of finer grain size and slightly larger bulk samples (~6–9 mg) for them.

The slope of an isochron regressed through the A881394 data gives initial ⁵³Mn/⁵⁵Mn = $(4.6 \pm 1.7) \times 10^{-6}$, and initial $\epsilon(^{53}\text{Cr})_I = 0.25 \pm 0.17$. These values are identical within their error limits to those for an isochron defined by data for bulk diogenites and eucrites [6]. The latter has been interpreted as dating the last global differentiation of the HED parent body. The initial ⁵³Mn abundance in A881394 also can be compared to initial ⁵³Mn/⁵⁵Mn = $(1.44 \pm 0.07) \times 10^{-6}$ for the angrite LEW86010 [3]. The formation interval for A881394 relative to the LEW86010 angrite thus obtained is $\Delta t_{\text{LEW}} = -6 \pm 2$ Ma. An ‘absolute’ Pb–Pb age of 4558 Ma was determined for LEW86010 [7] implying an ‘absolute’ age of 4564 ± 2 Ma for A881394.

The Mn–Cr data for the Asuka 881467 eucrite also satisfy an isochron relationship for ⁵³Mn/⁵⁵Mn = $(6.1 \pm 4.4) \times 10^{-7}$ and $\epsilon(^{53}\text{Cr})_I = 0.91 \pm 0.20$. The formation interval is thus relatively imprecisely constrained to lie in the range $\Delta t_{\text{LEW}} \sim 2$ –12 Ma corresponding to an absolute age $T = 4546$ –4556 Ma. Isochron fits to the data for the other two eucrites yield only lower limits to the formation intervals and upper limits to their ages of $T < 4559$ Ma and $T < 4548$ Ma for A87272 and A881388, respectively. These data suggest either that magmatism on the HED parent body persisted for at least ~15–20 Ma, or that post-crystallization heating events reequili-

brated the Cr isotopic composition among the mineral phases in some of the eucrites.

Radioactive decay of ^{26}Al was postulated to have supplied the heat to melt the asteroids [8]. If so, the very ancient age of A881394 implied by the Mn–Cr data shows it to be a good candidate in which to search for excess radiogenic $^{26}\text{Mg}^*$, evidence of the initial presence of ^{26}Al .

4. Al–Mg formation interval

Table 3 reports the Mg isotopic compositions of A881394 and three other Asuka eucrites, A87272, A881388, and A881467. The mineralogy of the latter three eucrites has been described previously [9]. The $^{26}\text{Mg}/^{24}\text{Mg}$ values are normalized to $^{25}\text{Mg}/^{24}\text{Mg} = 0.12663$ [10], and expressed as per mil (‰) deviations, $\delta(^{26}\text{Mg})$, from the terrestrial $^{26}\text{Mg}/^{24}\text{Mg}$ value determined for laboratory standards. The $^{26}\text{Mg}/^{24}\text{Mg}$ ratios were corrected for mass fractionation during analysis according to the exponential law [11]. Two series of analyses of the laboratory Mg standard performed contemporaneously with the sample analyses gave values of $^{26}\text{Mg}/^{24}\text{Mg} = 0.139420 \pm 15$ (35 analyses) and 0.139419 ± 29 (15 analyses), respectively. The quoted error limits refer to the last digits and are $\pm 2\sigma_p$, where σ_p is the population standard deviation. The quoted error limits for the meteorite data are either $\pm 2\sigma_p$ for several analyses of that sample, or $\pm 2\sigma_p$ for the series of contemporaneous standard analyses, whichever is greater. These error limits are more conservative than those used for the Cr isotopic analyses because the measured values of Mg isotopic composition vary with Al^+/Mg^+ during the analyses, asymptotically approaching ~ 0.13942 as Al^+/Mg^+ increases. The values obtained here for $^{26}\text{Mg}/^{24}\text{Mg}$ for the standard are within error limits of the ‘absolute’ value of 0.13932 ± 26 reported by Catanzaro et al. [10]. Seven analyses of the Mg standard at JSC following the procedure of [10] gave $^{26}\text{Mg}/^{24}\text{Mg} = 0.139395 \pm 25$. Ion yields for this procedure were too low for use with the meteorite samples, however. Because the measured Mg isotopic composition varies rapidly with Al^+/Mg^+ for low values of Al^+/Mg^+ , the Al^+/Mg^+ ratio is kept

within a selected operational range for both standard and sample analyses. The error limits are chosen to reflect the degree to which the measured Mg isotopic ratios are reproducible, and for this purpose, the population standard deviation, σ_p , is appropriate for both standard and sample analyses. In contrast, there is no evidence of non-random error terms in the Cr isotopic measurements. Error limits based on the standard deviation of the mean of the isotopic measurements are appropriate when comparing sample and standard Cr analyses.

Fig. 3 shows the Al/Mg data in an isochron

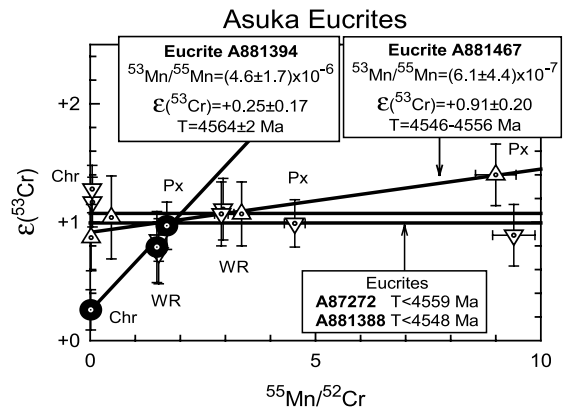


Fig. 2. Mn/Cr isochron for whole rock (WR), pyroxene (Px), and chromite (Chr) separates from granulitic magnesian eucrite Asuka 881394 compared to Mn–Cr data for three other eucrites. The slope of the isochron for A881394 gives $^{53}\text{Mn}/^{55}\text{Mn} = (4.6 \pm 1.7) \times 10^{-6}$, identical within error limits with $^{53}\text{Mn}/^{55}\text{Mn} = (4.7 \pm 0.6) \times 10^{-6}$ for the HED parent body at the time of its differentiation [6]. The intercept, $\epsilon(^{53}\text{Cr})_i = 0.25 \pm 0.17$, is also identical with initial $\epsilon(^{53}\text{Cr})_i = 0.25 \pm 0.07$ for the HED parent body [6], consistent with the O isotopic evidence [1] that A881394 derives from the same parent asteroid as the other HED meteorites. Data for two other eucrites, A87272 and A881388, show uniform enrichment of radiogenic $^{53}\text{Cr}^*$ in the analyzed phases, indicating that these eucrites either solidified after ^{53}Mn had decayed, or that the Cr isotopic composition was homogenized in them during post-crystallization thermal metamorphism. The data for a third eucrite, A881467, satisfy a relatively imprecisely defined isochron relationship for $^{53}\text{Mn}/^{55}\text{Mn} = (6.1 \pm 4.4) \times 10^{-7}$ and $\epsilon(^{53}\text{Cr})_i = 0.91 \pm 0.20$. The Mn–Cr formation interval, Δt_{LEW} , of A881394 relative to the LEW86010 angrite is -6 ± 2 Ma, implying initial crystallization of A881394 at 4564 ± 2 Ma ago, assuming an ‘absolute’ age, T , of 4558 Ma for the angrite [7]. For A881467, $\Delta t_{\text{LEW}} \sim 2$ –12 Ma and $T = 4546$ –4556 Ma. Upper limits on the ages of A87272 and A881388 are $T < 4559$ Ma and $T < 4548$ Ma, respectively.

Table 3
Al–Mg analytical data for Asuka eucrites A881394, A87272, A881388, and A881467

Sample ^a	Weight (mg)	Al (wt%)	Mg ^b (ppm)	²⁷ Al/ ²⁴ Mg ^c (%)	$\delta^{26}\text{Mg}^d$
(1) Eucrite A881394					
Plag1	4.6	18.8 ^e	819	261 ± 26	1.97 ± 0.11
Plag2a	1.3	18.8 ^e	918	233 ± 23	1.97 ± 0.11
Plag2b	1.13	18.8 ^e	937	228 ± 23	1.92 ± 0.15
Plag3a	7.35	18.9 ^f	1064	203 ± 10	1.72 ± 0.11
I-Plag3b (impure)	8.66	18.5 ^f	1198	176 ± 9	1.18 ± 0.11
Px1	1.77	0.30 ^e	96900	0.04 ± 0.01	−0.05 ± 0.34
Px2	0.73	0.30 ^e	93300	0.04 ± 0.01	0.01 ± 0.28
(2) Eucrite A87272					
Plag	8.56	18.4 ^f	1731	121 ± 6	−0.03 ± 0.21
I-Plag	9.5	14.7 ^f	13040	12.8 ± 0.6	−0.12 ± 0.21
Px	6.01	0.60 ^f	65100	0.10 ± 0.01	−0.07 ± 0.21
(3) Eucrite A881388					
Plag	5.44	19.6 ^f	1516	147 ± 7	−0.04 ± 0.21
I-Plag	4.16	18.0 ^f	9630	21.3 ± 1.1	−0.06 ± 0.21
Px	6.12	0.96 ^f	65780	0.17 ± 0.01	0.02 ± 0.21
(4) Eucrite A881467					
Plag1	2.42	17.3 ^f	2462	80.1 ± 4.0	0.07 ± 0.21
Plag2	5.53	19.3 ^f	2660	83.0 ± 4.1	−0.01 ± 0.21
Px1A	1.61	0.39 ^f	69400	0.07 ± 0.01	−0.08 ± 0.21
Px1B	1.16	0.90 ^f	54960	0.18 ± 0.01	−0.02 ± 0.21

^a Plag = plagioclase, I-Plag = impure plagioclase, Px = pyroxene.

^b Determined by isotopic dilution using a ²⁵Mg spike.

^c Error limits are ± 5% and ± 10% for inductively coupled plasma-source mass spectrometry (ICP-MS) and EPMA analyses, respectively.

^d $\delta^{26}\text{Mg}(\text{‰}) = 1000 \times [(\text{Mg}^{26}/\text{Mg}^{24})_{\text{sample}} / (\text{Mg}^{26}/\text{Mg}^{24})_{\text{standard}} - 1]$. ²⁶Mg/²⁴Mg in the terrestrial standard = 0.139420 ± 0.000015 normalized to ²⁵Mg/²⁴Mg = 0.12663 [10] for 35 runs of the standard during the A881394 analyses and 0.139419 ± 0.000029 for 15 runs during analysis of the other three eucrites. The error limits for the standard analyses refer to the last digits and are twice the standard deviation of the population of values obtained within a given series of analyses (± 2 σ_p). The error limits for the samples are the greater of ± 2 σ_p for several sample runs, or ± 2 σ_p of the standard runs.

^e Determined by EPMA (Table 1).

^f Determined by ICP-MS (analyst: C.M. Kuo, Wyle Laboratories).

plot. For A881394, $\delta^{26}\text{Mg}$ values correlate with ²⁷Al/²⁴Mg values, whereas there are no detectable ²⁶Mg excesses for the other three eucrites. The A881394 data determine an Al–Mg isochron with a slope corresponding to initial ²⁶Al/²⁷Al = (1.18 ± 0.14) × 10^{−6}, from which a forma-

tion interval, Δt_{CAI} , of 3.95 ± 0.13 Ma can be calculated relative to the canonical value of ²⁶Al/²⁷Al = 5 × 10^{−5} for Allende CAI [12,13]. Here we use an ²⁶Al half-life of 0.73 Ma following a convention established for Al–Mg studies [13,14], although a lower value of 0.705 ± 0.024 Ma [15] is in common use in cosmogenic nuclide studies [16]. Nishiizumi [16] summarized recent determinations of the ²⁶Al half-life for which a weighted average is 0.715 ± 0.016 Ma. Using the 0.705 Ma value preferred by [16] would change the formation interval to 3.81 ± 0.13 Ma, a change comparable to the statistical uncertainty.

The Mg isotopic data for the other eucrites analyzed simultaneously with A881394 (Table 3, Fig. 3) show no evidence of ²⁶Mg excesses. The ²⁷Al/²⁴Mg ratios for their plagioclase separates are lower than those for the A881394 plagioclase separates, but are similar to those reported by Srinivasan et al. [17] for plagioclase separates of the Piplia Kalan eucrite. The ²⁷Al/²⁴Mg ratios for all the plagioclase separates are much lower than values of ~ 5000 obtained by in situ SIMS analyses of plagioclase in Piplia Kalan [18].

The Al–Mg formation interval of A881394 can be combined with the ‘absolute’ Pb–Pb age of CAI to obtain an estimate of the absolute age of A881394 that is analogous to that derived from its Mn–Cr formation interval. The customarily assumed Pb–Pb age of CAI of ~ 4566 Ma [14,19] combined with the Al–Mg formation interval gives ~ 4562 Ma as the age of A881394. Recently, Amelin et al. [20] have reported the Pb–Pb age of CAI from the CV chondrite Efremovka to be 4567.2 ± 0.6 Ma. They also report initial ²⁶Al/²⁷Al = (4.63 ± 0.44) × 10^{−5} for one of the CAI, E60. Accepting the latter value as equivalent to the ‘canonical’ ²⁶Al/²⁷Al value (as do Amelin et al.) leads to an estimated absolute age of 4563.2 ± 0.6 Ma for A881394, in excellent agreement with the age estimated from the Mn–Cr systematics and the Pb–Pb age of the angrite LEW86010. In earlier work, Lugmair and Shukolyukov [21] argued that the ~ 4566 Ma age for CAI is inconsistent with the time of other early solar system events, and placed CAI formation at ~ 4571 Ma. In that case, the absolute crystallization age of A881394 would be ~ 4567 Ma. This

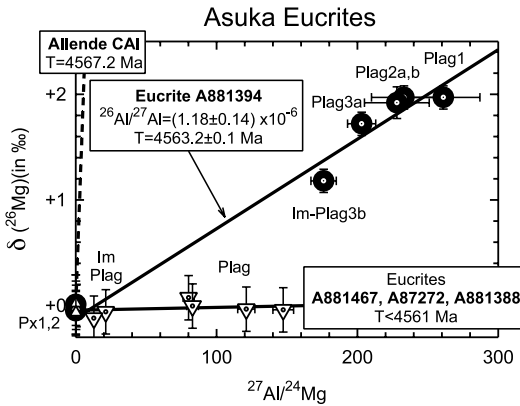


Fig. 3. Al/Mg isochron for plagioclase and pyroxene separates from granulitic magnesian eucrite Asuka 881394. The slope of the isochron gives initial $^{26}\text{Al}/^{27}\text{Al} = (1.18 \pm 0.14) \times 10^{-6}$, and a formation interval, Δt_{CAI} , of 3.95 ± 0.13 Ma relative to the canonical value of $^{26}\text{Al}/^{27}\text{Al} = 5 \times 10^{-5}$ for Allende CAI [12,13]. This formation interval combined with an ‘absolute’ Pb–Pb age of 4567.2 Ma for CAI [20] gives $T = 4563.2 \pm 0.1$ Ma as the absolute crystallization age of A881394. The error limit is increased to 0.6 Ma when the uncertainty of the Pb–Pb age is included. Plagioclase and pyroxene data for a series of basaltic eucrites, A881467, A87272, and A881388, show no enrichment of radiogenic $^{26}\text{Mg}^*$ in plagioclase, indicating that these eucrites either solidified after ^{26}Al had decayed, or that the Mg isotopic composition was homogenized in them during post-crystallization thermal metamorphism.

age is marginally higher than the 4564 ± 2 Ma age derived from the Mn–Cr systematics and the Pb–Pb age of LEW86010.

Fig. 4 illustrates how determining both Al–Mg and Mn–Cr isochrons for A881394 allows these two short-lived chronometers to be calibrated to one another and to an absolute age standard. Beginning with the ‘absolute’ Pb–Pb age of ~ 4558 Ma for LEW86010 [7], the Mn–Cr formation interval $\Delta t_{\text{LEW}} = -6 \pm 2$ Ma, places formation of A881394 at $\sim 4564 \pm 2$ Ma before the present, neglecting the uncertainty in the reference age. Adding the CAI-to-A881394 Al–Mg formation interval, $\Delta t_{\text{CAI}} = 3.95 \pm 0.13$ Ma, places CAI formation at $\sim 4568 \pm 2$ Ma in turn. As noted above, this derived CAI age is in good agreement with the Pb–Pb age directly determined for CAI by Amelin et al. [20]. Mn–Cr data for chondrules from the Chainpur and Bishunpur unequilibrated ordinary chondrites (UOC) show that chondrules

were forming in the solar nebula with initial $^{53}\text{Mn}/^{55}\text{Mn} \sim 9.5 \times 10^{-6}$ [22] about 4 Ma prior to differentiation of the HED parent body and formation of A881394. A recent investigation of five ferromagnesian chondrules from the Semarkona UOC gave initial $^{26}\text{Al}/^{27}\text{Al}$ values averaging $(7.86 \pm 1.43) \times 10^{-6}$ [23]. The formation interval of these chondrules relative to $^{26}\text{Al}/^{27}\text{Al}$ in A881394 is -1.9 ± 0.3 Ma. One chondrule from the Efremovka CV3 chondrite gave a higher initial $^{26}\text{Al}/$

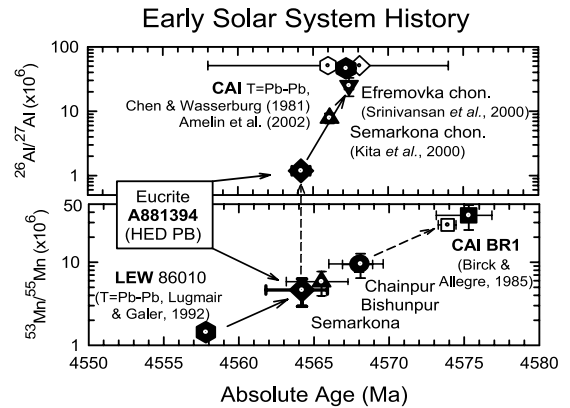


Fig. 4. Formation chronology for angrite LEW86010, eucrite A881394, chondrules, and CAI. The horizontal axis gives ‘absolute’ age in Ma. For LEW86010 and CAI, Pb–Pb ages [7,19,20] are assumed to be ‘absolute’ ages. For the other samples, ‘absolute’ ages are calculated from the Mn–Cr and Al–Mg formation intervals referenced to the Pb–Pb age of the angrite [7]. The vertical axes give $^{26}\text{Al}/^{27}\text{Al}$ (upper panel) and $^{53}\text{Mn}/^{55}\text{Mn}$ (lower panel) on logarithmic scales. The common Mn–Cr formation interval of ~ 6 Ma for A881394 and bulk eucrites and diogenites [6] relative to LEW86010 places differentiation of the HED parent body at ~ 4564 Ma ago. The Al–Mg data for A881394 suggest CAI formed with the canonical value of $^{26}\text{Al}/^{27}\text{Al} = 5 \times 10^{-5}$ about 4 Ma earlier, at ~ 4568 Ma (open diamond in top panel), within analytical uncertainties of the Pb–Pb ages of CAI. The dated CAI are from the CV3 chondrites Allende ([19], open hexagon) as reviewed by [14], and Efremovka ([20], solid hexagon). The error limits for the Efremovka CAI Pb–Pb age [20] are contained within the symbol. Absolute ages of chondrules from Efremovka ([24], inverted triangle) and Semarkona ([23], triangle) are calculated from their Al–Mg formation intervals relative to A881394. The Mn–Cr data for bulk chondrules from Chainpur and Bishunpur [22] as well as Semarkona (unpublished JSC data) are consistent with the Al–Mg timescale for chondrules. Mn–Cr data implying formation of CAI at ~ 4574 – 4575 Ma (dashed arrow, squares) apparently reflect lack of complete Cr isotopic equilibration in the early solar nebula.

$^{27}\text{Al} = (2.5 \pm 0.8) \times 10^{-5}$ [24], indicating formation at 3.2 ± 0.3 Ma prior to A881394. The Al–Mg data for these chondrules agree well with the Mn–Cr timescale, but initial $^{53}\text{Mn}/^{55}\text{Mn} = (2.8 \pm 0.3) \times 10^{-5}$ [22], or $(3.66 \pm 1.22) \times 10^{-5}$ [25] for CAI places the CAI-to-A881394 interval at 9.6 ± 2.5 Ma, and CAI formation at ~ 4574 Ma. The unresolved inconsistency between Al–Mg and Mn–Cr chronometry for CAI is attributed most readily to lack of isotopic homogenization between Cr in very refractory spinels in CAI and the bulk of the Cr in the solar nebula. As will be discussed later in the paper, formation of the HED parent body contemporaneously with chondrules having ^{26}Al abundances like those given would have resulted in its melting from the energy released in radioactive decay of the ^{26}Al .

Srinivasan et al. [17,26,27] reported radiogenic $^{26}\text{Mg}^*$ excesses in the eucrite, Piplia Kalan, but the initial abundances determined for the longer-lived activities ^{53}Mn and ^{146}Sm in Piplia Kalan [17,27] are inconsistent with the reported initial abundances of $^{26}\text{Al}/^{27}\text{Al}$ of $\sim (0.8\text{--}2.6) \times 10^{-6}$. For example, an upper limit to initial $^{53}\text{Mn}/^{55}\text{Mn} < 1.9 \times 10^{-6}$ [17] implies ‘formation’ of Piplia Kalan or its protolith ~ 4.7 Ma after differentiation of the HED parent body. During this time interval, equivalent to ~ 6.5 half-lives of ^{26}Al , the ^{26}Al abundance would have fallen to $\sim 1\%$ of its initial abundance, i.e. to $< \sim 5 \times 10^{-7}$, even if the HED parent body initially contained the canonical abundance of ^{26}Al , i.e. $^{26}\text{Al}/^{27}\text{Al} = 5 \times 10^{-5}$. Also, initial $^{146}\text{Sm}/^{144}\text{Sm} = (4.4 \pm 1.2) \times 10^{-3}$ for Piplia Kalan [27] corresponds to a $^{146}\text{Sm}\text{--}^{142}\text{Nd}$ formation interval, $\Delta t_{\text{LEW}} = 81 \pm 36$ Ma, and implies formation of Piplia Kalan at least ~ 60 half-lives of ^{26}Al after crystallization of the LEW86010 angrite. That the short-lived radiometric systems of Piplia Kalan give results that are ‘not easily reconcilable’ [27] may be because Piplia Kalan is a genomet breccia [28] that probably was assembled from a more ancient lithology at the $^{39}\text{Ar}\text{--}^{40}\text{Ar}$ age of ~ 3.6 Ga [29]. Thermal processing during assembly of Piplia Kalan could have partially homogenized pre-existing isotopic heterogeneities in rocks of the protolith. In contrast, the granulitic texture of Asuka 881394 can be related to the igneous texture of

the original crystalline rock, and radiogenic enrichments in $^{26}\text{Mg}^*$ can be considered to have been generated in situ.

SIMS analyses by Srinivasan [30] confirmed the presence of excess $^{26}\text{Mg}^*$ in A881394 plagioclase corresponding to initial $^{26}\text{Al}/^{27}\text{Al} = (2.1 \pm 0.4) \times 10^{-6}$. This value is nearly a factor of two higher than we found, and suggests that A881394 could be ~ 0.6 Ma older than our data indicate. Srinivasan [30] also reported that the $^{26}\text{Mg}^*$ excesses were not well correlated with Al/Mg ratios in plagioclase. The $^{27}\text{Al}/^{24}\text{Mg}$ ratios measured in situ by SIMS were about twice those measured for our mineral separates, but the analytical uncertainties illustrated for the isotopic measurements were $\sim 7\%$ [30], about six times larger than for the TIMS data. For some analyses, the analytical uncertainties of the SIMS isotopic data are comparable to the measured $^{26}\text{Mg}^*$ excesses [30]. Because our own data do not show evidence of disturbance of the isochron relationship between $^{26}\text{Mg}^*$ and $^{27}\text{Al}/^{24}\text{Mg}$, we will not attempt to explore the possible implications of a disturbed Al–Mg system here.

Srinivasan [31] also reported that eucrites A87122 and Vissananepta contain excess $^{26}\text{Mg}^*$. The initial $^{26}\text{Al}/^{27}\text{Al}$ values of those meteorites, $(5.7 \pm 4.2) \times 10^{-7}$ and $(1.03 \pm 0.46) \times 10^{-6}$, respectively, are close to our value for A881394, but apparently extend the record of magmatism in the presence of live ^{26}Al on the HED parent body by an additional ~ 1 Ma. The longer-lived ^{53}Mn extends the recorded magmatic period to $\sim 15\text{--}20$ Ma after CAI, as typified by A881467 and some other eucrites [14]. One must look to the long-lived chronometers to determine when magmatism on the HED parent body may have ceased.

5. Preservation of radiogenic $^{26}\text{Mg}^*$ excesses in A881394

The granulitic texture of A881394 formed after its igneous crystallization, and thus raises the question: why was not the Mg isotopic composition rehomogenized then? During recrystallization, radiogenic $^{26}\text{Mg}^*$ would have diffused out

of plagioclase, and non-radiogenic ^{26}Mg would have diffused in, tending to reset the Al–Mg clock. If recrystallization immediately followed initial crust formation, and if it was rapid and close to the time of parent body formation, radiogenic $^{26}\text{Mg}^*$ could have reaccumulated. In that case, the Al–Mg isochron would date the recrystallization.

Partial Sr and Nd isotopic reequilibration is required to account for the comparatively low and discordant Rb–Sr and Sm–Nd ages of 4370 ± 60 Ma and 4490 ± 20 Ma for A881394 [2], however, and may imply partial Mg isotopic reequilibration. LaTourette and Wasserburg [32] found $(D/a^2)_{\text{Mg}}$ to be $\sim 100 \times (D/a^2)_{\text{Sr}}$ in anorthite, suggesting that Mg isotopic reequilibration would be greater than Sr isotopic reequilibration. However, the relationship between $(D/a^2)_{\text{Mg}}$ and $(D/a^2)_{\text{Sr}}$ appears to be reversed in vitreous albite [33], suggesting some uncertainty in the relative magnitudes of these quantities. Additionally, recrystallization might have hindered Mg isotopic equilibration. For example, if radiogenic $^{26}\text{Mg}^*$ cations stayed at the tetrahedral sites of the plagioclase framework structure following ^{26}Al decay, their diffusion rate might be slow in comparison to cations located outside the framework. Also, the short ^{26}Al half-life makes the absolute error of an Al–Mg formation interval very much smaller than the error caused by an equivalent degree of isotopic reequilibration of one of the long-lived chronometers. That is, any remnant of excess $^{26}\text{Mg}^*$ remaining after partial isotopic equilibration would nevertheless be interpreted as indicating a formation interval of only a few million years. The preservation of an equivalent percentage change in age from 4564 Ma, for example, would require long-lived isotope chronometers to show essentially no evidence of isotopic equilibration. Thus, over the age of A881394, the Al–Mg chronometer could appear robust compared to the Rb–Sr and Sm–Nd chronometers.

6. Was the ^{26}Al abundance in A881394 enough to melt its parent body?

Eq. 1 from Schramm et al. [34] gives the heat,

H_0 , produced in each gram of a parent body due to ^{26}Al decay as:

$$H_0 \text{ (cal/g/yr)} = 4.8 \times 10^{-4} (^{26}\text{Al/Si}). \quad (1)$$

The ^{26}Al abundance used here is the atomic abundance per 10^6 Si atoms. With the assumption that no heat is lost from the asteroid, the maximum increase of its central temperature, $(T_C - T_0)$, was estimated to be:

$$(T_C - T_0) \sim (H_0 \tau / C_p) \quad (2)$$

where T_0 is the initial temperature, C_p is the specific heat capacity, and $\tau = 1/\lambda$ is the mean lifetime of ^{26}Al for decay constant λ . Using $C_p = 0.2$ cal/g/deg, $^{26}\text{Al}/^{27}\text{Al} = 1.18 \times 10^{-6}$, and an atom ratio Al/Si = 0.069 for the HED parent body for the average estimated composition [35], gives a maximum estimated temperature increase $(T_C - T_0)$ of only 203°C. Assuming, as Schramm et al. [34] did, an initial temperature of 100 K, the maximum estimated central temperature of the asteroid would be ~ 303 K, far short of that required for melting.

In a more elaborate thermal model, Ghosh and McSween [36] chose an initial temperature of 292 K for Vesta, but even for this choice, the central temperature calculated for the asteroid with the above conditions is only 495 K, and also falls short of that needed for melting. From Eq. 2, the estimated ^{26}Al abundance needed to attain a central temperature $T_C \sim 1443$ K (1170°C), an approximate melting temperature (solidus) for basalts like A881394, is $^{26}\text{Al}/^{27}\text{Al} = 7.8 \times 10^{-6}$, for an initial temperature, $T_0 \sim 100^\circ\text{C}$. The thermal model of LaTourette and Wasserburg [32] includes surface heat loss [37], omitted from the model of Schramm et al. [34]. It leads to interior melting ~ 4 Ma after CAI formation for a Vesta-sized asteroid 265 km in radius that formed with the bulk composition estimated by Warren [35] and initial $^{26}\text{Al}/^{27}\text{Al} = 6.7 \times 10^{-6}$. It requires a slightly higher initial $^{26}\text{Al}/^{27}\text{Al} = 7.1 \times 10^{-6}$ for melting within ~ 25 km of the surface at that time. These values agree remarkably well with the $^{26}\text{Al}/^{27}\text{Al}$ values found for ferromagnesian chondrules from UOC, but are more than twice the initial $^{26}\text{Al}/^{27}\text{Al}$ value of 3.22×10^{-6} used by Ghosh and McSween [36] for their Vesta thermal model. Those authors assumed an asteroid of

H-chondritic bulk composition with an Al/Si ratio nearly the same as for the HED parent body composition of Warren [35]. Also, the model of Ghosh and McSween [36] considers redistribution of heat sources during melting, a fundamental difference between it and the simple models used here.

One can ‘calibrate’ Eq. 2 to give the same temperature change, $(T_C - T_0) = 931^\circ\text{C}$, as in the Ghosh and McSween model [36] for their Stage 1, which ends with core formation at 1223 K. This requires a multiplicative factor 1.7, effectively extending the heating interval in Eq. 2 from τ to 1.7τ . The corresponding estimated ^{26}Al abundance needed to bring the center of the asteroid to melting temperature from 292 K is lowered to $^{26}\text{Al}/^{27}\text{Al} \sim 4.0 \times 10^{-6}$, similar to the value of $\sim 3.2 \times 10^{-6}$ used in the Ghosh and McSween [36] model. The estimated time interval from accretion of the HED parent body to crystallization of A881394 with $^{26}\text{Al}/^{27}\text{Al} = 1.18 \times 10^{-6}$ is 1.96 Ma if the parent body initial $^{26}\text{Al}/^{27}\text{Al} = 7.8 \times 10^{-6}$, and 1.27 Ma if the initial $^{26}\text{Al}/^{27}\text{Al} = 4.0 \times 10^{-6}$, respectively. The corresponding interval in the Ghosh and McSween model [36] from parent body formation to crust formation at the end of their Stage 2 is 3.7 Ma. All of these time intervals are roughly similar, suggesting that the ^{26}Al abundance in A881394 could be consistent with the higher values needed to initiate parent body melting. However, none of the models suggests that the ^{26}Al abundance inferred from the presence of excess radiogenic $^{26}\text{Mg}^*$ in A881394 would have been sufficient in itself to melt the HED parent body.

7. Consistency between the ^{26}Al timescale and estimated accretion timescales

If the HED parent body is the asteroid 4 Vesta, then the ^{26}Al timescale implies that mm-sized chondrules and other dust accreted into a body of mass $m \sim 10^{23}$ g and radius ~ 265 km, was melted, and chemically differentiated within ~ 2 –4 Ma. The preceding discussion assumes an already-accreted asteroidal body, and shows that melting and initial differentiation alone likely re-

quired ~ 1 –4 Ma. Are these results consistent with theoretically estimated accretion timescales? Greenberg et al. [38] numerically simulated the growth of ‘planets’ ~ 500 km in diameter from an initial swarm of 1 km-sized planetesimals. They concluded that bodies in sizes up to ~ 20 km in diameter would accrete within a few hundred years, bodies ~ 500 km in diameter would accrete within ~ 6000 yr, and bodies ~ 1000 km in diameter would accrete within ~ 16000 yr. Such rapid accretion times allow adequate time for subsequent melting and differentiation of the accreted bodies. But, if asteroidal-sized bodies accreted so rapidly, why were not all asteroids above a threshold size melted by ^{26}Al decay?

The work of Nakagawa et al. [39], for example, suggests accretion occurred at a more leisurely pace. They give the characteristic time, T_G , for planetary bodies to grow as $T_G \sim m^{1/3} R^3$, i.e. the growth rate varies with radial distance, R , from the sun. They found T_G for a body of mass $m \sim 10^{23}$ g in earth orbit to be $\sim 2 \times 10^5$ yr. If Vesta accreted near its present orbit at ~ 2.36 AU, its accretion rate would be slowed relative to a similar body in earth orbit by the factor $(2.36)^3$, i.e. T_G would be $\sim 2.6 \times 10^6$ yr. However, a numerical simulation by the same authors [39] suggests somewhat more rapid growth. That is, their numerical simulation suggested that a body in earth orbit could grow to $\sim 10^{24}$ g within $\sim 2 \times 10^5$ yr. This implies that the actual growth time, T_G' , for a body of a given size would be approximated by T_G for a smaller body. Nakagawa et al. [39] did not present the results of numerical simulations for $m < 10^{24}$ g, but one might infer from the foregoing example that $T_G \sim 10^6$ yr calculated for $m \sim 10^{22}$ g might be close to the actual time, T_G' required to grow to a Vesta-sized body with $m \sim 10^{23}$ g. Another estimate can be obtained from the work of Wetherill [40], who numerically simulated the growth of bodies at 2.5 AU from the sun. A largest body 624 km in diameter was ‘accreted’ in 10^6 yr. Thus, accretion of Vesta could have occupied a significant portion of the ~ 2 Ma time interval between the time when $^{26}\text{Al}/^{27}\text{Al}$ was $\sim 7.86 \times 10^{-6}$ in ferromagnesian chondrules [23] and the time when $^{26}\text{Al}/^{27}\text{Al}$ was $\sim 1.18 \times 10^{-6}$ in A881394.

The short half-life of ^{26}Al would have made it an ephemeral heat source. Compare another minor planet, 1 Ceres, having mass $m \sim 6 \times 10^{23}$ g, and located at $R = 2.77$ AU. Using the relationship of Nakagawa et al. [39], the characteristic growth time of 1 Ceres, $T_{G,1}$, exceeds that of 4 Vesta, $T_{G,4}$, by the factor 2.9, i.e. $T_{G,1} = 2.9 T_{G,4}$. Thus, for $T_{G,4} \sim 1$ Ma for 4 Vesta, $T_{G,1} \sim 3$ Ma for 1 Ceres. Even for accretion to a Vesta-sized mass of 10^{23} g, the time required at the orbit of Ceres would exceed that at the orbit of Vesta by a factor 1.6, i.e. $T_{G,1}$ ($R = 2.77$ AU, $m = 10^{23}$ g) = 1.6 $T_{G,4}$ ($R = 2.36$ AU, $m = 10^{23}$ g). Thus, if $T_{G,4} \sim 1$ Ma, $T_{G,1} \sim 1.6$ Ma, i.e. accretion of Ceres would be delayed by nearly one half-life of ^{26}Al . A two-fold decrease in ^{26}Al abundance from $^{26}\text{Al}/^{27}\text{Al} \sim 4.0 \times 10^{-6}$, estimated to be required for melting using the method of Schramm et al. [34] as ‘calibrated’ above, would cause a decrease of $(T_C - T_0)$ from $\sim 1150^\circ\text{C}$ to $\sim 575^\circ\text{C}$, inadequate for melting. Thus, although some incipient radiogenic melting may have occurred in the first-accreted material, it is likely the ^{26}Al abundance in later-accreted material would be too low for radiogenic melting. Similar considerations apply to 2 Pallas. Both asteroids have surface mineralogies suggesting that they are undifferentiated [41], possibly as a result of tardy accretion.

Grimm and McSween [42] applied similar reasoning to present isotherms for temperatures from 0°C to 1100°C as a function of asteroid diameter and orbital radius or time of accretion, respectively. They estimated, for example, that on average asteroids > 100 km diameter would reach temperatures above the melting point of ice and silicate, respectively, inward of ~ 3.4 AU (ice), and ~ 2.7 AU (silicate), respectively.

8. Role of accretional heating

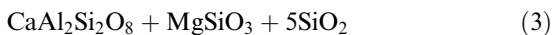
Accretional heating could have augmented ^{26}Al heating during the final stages of asteroid formation. Moreover, petrological considerations suggest it may have been difficult to produce eucrites as magnesian as A881394 if ^{26}Al were the only heat source for melting. Partial melting due to ^{26}Al heating and beginning in the interior of the

parent body would cause comparatively iron-rich lavas such as ordinary basaltic eucrites with low values of molar $\text{Mg}/(\text{Mg}+\text{Fe}) = 0.30\text{--}0.42$ [43], to be erupted to the surface of the parent body. The higher $\text{mg}' = \text{Mg}/(\text{Mg}+\text{Fe}) = 0.57$ for A881394 [4,44] suggests it formed differently. Such high mg' values are typical for angrites and cumulate eucrites, but A881394 does not have the composition of an angrite [4,44], or pyroxene exsolution textures [9] like those of typical cumulate eucrites, so its petrogenesis must have differed from that of those rock types, also.

Late-stage accretion could have supplied relatively magnesian primordial material to the surface of the parent body as well as providing additional incremental heating. A shallow magma ocean accompanied by a thin veneer (scum layer) of comparatively Mg-rich composition might have covered the surface of the parent body, as proposed by Ikeda and Takeda [45]. These authors found olivine fragments with $\text{mg}' = 0.88\text{--}0.71$ and diogenite clasts with mg' up to 0.76 in the Yamato 7308 howardite. They argued that these fragments and clasts could have coexisted with a single primary liquid of evolving composition from $\text{mg}' \sim 0.70$ to ~ 0.46 for olivine crystallization and $\text{mg}' \sim 0.46$ for crystallization of olivine plus pyroxene. Saiki et al. [46] also considered the relationship between mg' in pyroxenes and coexisting equilibrium liquids for a variety of eucritic and diogenitic clasts in the polymict eucrite Y791192. They found diogenites with mg' up to ~ 0.68 that apparently crystallized from primary liquids with $\text{mg}' \sim 0.36$, assuming the pyroxene/liquid distribution coefficient $K_D = 0.27$ [45] instead of 0.30 [46]. The higher value of $\text{mg}' = 0.57$ for A881394 suggests that it could have solidified from the primary magma at a more primitive stage of evolution, possibly including some cumulus pyroxene. Early solidification of A881394 is consistent with the presence of ^{26}Al , and could be consistent with its inclusion within the thin ‘scum’ layer that Ikeda and Takeda [45] hypothesized as covering a shallow magma ocean on the HED parent body. As discussed by them, an initial composition of the magma ocean having $\text{mg}' \sim 0.70$ would be required to account for crystallization of olivine and orthopyroxene with high

mg' from it. Partial melts of the interior would have had lower mg' values of ~ 0.30 – 0.42 as typical of ordinary basaltic eucrites. Thus, late-stage accretion of primitive material may have been required to keep a magma ocean on the HED parent body sufficiently magnesian to account for the presence of olivine and orthopyroxene with high mg' numbers in surface breccias from it.

The hypothetical early-formed, thin, outer crust of the HED parent body might have been kept hot after ^{26}Al had mostly decayed by heat from the magma beneath it. Intense bombardment by meteoroids onto the early crust, during the last stages of accretion, would be a favorable environment for Na volatilization, accounting for the most important and unusual mineralogical feature of A881394: the very calcic nature of its plagioclase. Yamaguchi et al. [47] performed shock experiments on evacuated, pre-heated eucrites, and found that Na loss was observed in shock melts for those samples pre-heated at 863°C and shocked at 23 GPa. An implication of this experiment is that one can expect Na loss by repeated impacts into a magma ocean with a thin, hot crust. Additionally, if one assumes chondritic source materials, eucritic compositions appear to be too calcic to represent direct partial melts. A possible chondritic partial melt found in the Caddo County IAB iron is unlike eucrites [48] and one of the authors (H.T.) proposed that the HED magma ocean may have been richer in albitic and diopsidic components than eucrites [43]. If we accept this proposal, the unusually low Na abundance in A881394 suggests that Na may have been lost by catastrophic bombardment during late-stage accretion to produce silica, magnesian pyroxene, and anorthite according to the equation:



This Na loss is consistent with the presence of very calcic plagioclase, abundant (5%) silica mineral in A881394, and magnesian pyroxenes. Yamaguchi et al. [49] also reported silica in EET90020, but this eucrite contained fayalite (Fe_2SiO_4), and their discussion cannot be applied

to A881394. Very early formation of such an outer crust would account for generation of radiogenic $^{26}\text{Mg}^*$ within it. Crystallization of large plagioclase grains, followed by recrystallization to smaller granulitic grains, would retard diffusion of ^{26}Mg out of the entire assemblage.

Yamaguchi et al. [50] considered eucrite metamorphism in a thermal environment accompanying rapid volcanism on an initially hot parent body. A881388, with no evidence of live ^{26}Al , was proposed to be a product of such metamorphism [50]. In the context of their model, the above scenario would occur before the major phase of volcanism. Relatively thin exsolution textures and the presence of uninverted pigeonites suggest that a parental mass of A881394 was excavated from the thin crust allowing significant cooling of the mass, locking radiogenic $^{26}\text{Mg}^*$ from ^{26}Al decay into plagioclase crystals. The granulitic texture of A881394 might have been produced during metamorphism in the thin crust on the magma ocean.

Thus, textural and mineralogical evidence suggests late, incremental, heating of asteroid 4 Vesta may have been supplied by the gravitational energy of accretion of its outermost layers. A similar scenario of combined radiogenic and accretional heating has been proposed by Ghosh et al. [51] to account for the possibility of early melting of Mars. Such scenarios appear to require a delicate balance between the time of onset of accretion and the rate of accretion. In the Martian case, formation of a magma ocean, distinguished from whole body melting, required that accretion begins more than ~ 2 Ma after CAI formation, and be completed within ~ 1 Ma [51]. An appropriately adjusted scenario appears reasonable for Vesta, also.

9. Conclusions

The abundance of ^{26}Al in A881394 during crystallization would have been sufficient to raise the internal temperature of an asteroidal parent body by only $\sim 200^\circ\text{C}$ if characteristic of the entire asteroid. From Eqs. 1 and 2 an approximately six-fold higher abundance would be required to

raise the internal temperature of an asteroid by $\sim 1200^\circ\text{C}$, sufficient for melting, from an initial temperature close to 0°C . Similar ^{26}Al abundances, i.e. $\sim 7.2 \times 10^{-6}$, have been observed in some chondrules present in primitive meteorites [23]. If the HED parent body formed contemporaneously with chondrules, it would have contained enough ^{26}Al for internal melting. This would require parent body formation earlier than A881394 by only about three half-lives of ^{26}Al , i.e. ~ 2 Ma. The thermal model of Ghosh and McSween [36] shows an even lower initial abundance of $^{26}\text{Al}/^{27}\text{Al} \sim 3.2 \times 10^{-6}$ could have been sufficient for partial melting of a Vesta-sized asteroid. Thus, ^{26}Al decay probably was a major contributor of the heat required for magmatism on the parent body of A881394, although it may not have been the only heat source. Even if the ^{26}Al abundance were insufficient for global melting, ^{26}Al decay would have produced a relatively hot asteroidal interior on which a global magma ocean could have been produced with minimal additional gravitational accretional energy.

If, as seems likely, A881394 indeed comes from asteroid 4 Vesta, differentiation of, and crustal formation on, this ‘smallest terrestrial planet’ appears to have been aided by radioactive decay of now-extinct ^{26}Al included in it during its accretion in the inner region of the asteroid belt. Furthermore, if ^{26}Al decay was the major heat source for asteroidal melting, it could have accounted for declining post-accretional heating in the asteroid belt with increasing solar distance and decreasing planetesimal size [42,52].

Acknowledgements

We thank the Antarctic Meteorite Research Center, National Institute of Polar Research, Tokyo, Japan, for providing us with the sample and Mrs. Mayumi Otsuki and Dr. T. Ishii for making elemental distribution maps of A881394 at the Ocean Research Institute, University of Tokyo. We also thank Dr. K. Yanai of Iwate University and Prof. R.N. Clayton of the University of Chicago for verification that the oxygen isotopic composition of Asuka 881394 is that of a eucrite.

We are indebted to Drs. A. Yamaguchi, T. Mikouchi, D. Bogard, P.C. Buchanan, G. McKay, D. Mittlefehldt, and Prof. Y. Ikeda for discussions, and to G. Srinivasan and A. Shukolyukov for helpful reviews. Financial support was provided via NASA RTOP 344-31-30-21 and a Grant-in-Aid for Scientific Research from the Japanese Ministry of Education, Science and Culture. This work was carried out as a part of ‘Ground Research Announcement for Space Utilization’ promoted by the Japan Space Forum. [KF]

References

- [1] K. Yanai, R.N. Clayton (personal communication).
- [2] L.E. Nyquist, Y. Reese, H. Wiesmann, C.-Y. Shih, H. Takeda, Live ^{53}Mn and ^{26}Al in an unique cumulate eucrite with very calcic feldspar ($An \sim 98$) (abstract), Meteorit. Planet. Sci. 36 (2001) A151–A152.
- [3] L.E. Nyquist, B. Bansal, H. Wiesmann, C.-Y. Shih, Neodymium, strontium and chromium isotopic studies of the LEW86010 and Angra dos Reis meteorites and the chronology of the angrite parent body, Meteoritics 29 (1994) 872–885.
- [4] K. Yanai, H. Kojima, Chemical compositions of the Antarctic meteorites, Cat. Antarct. Met. NIPR Tokyo (1995) 43–76.
- [5] W.R. Shields, T.J. Murphy, E.J. Catanzaro, E.L. Garner, Absolute isotopic abundance ratios and the atomic weight of a reference sample of chromium, J. Res. Nat. Bur. Stand. 70A (1966) 193–197.
- [6] G.W. Lugmair, A. Shukolyukov, Early solar system time-scales according to ^{53}Mn – ^{53}Cr systematics, Geochim. Cosmochim. Acta 62 (1998) 2863–2886.
- [7] G.W. Lugmair, S.J.G. Galer, Age and isotopic relationships among the angrites Lewis Cliff 86010 and Angra dos Reis, Geochim. Cosmochim. Acta 56 (1992) 1673–1694.
- [8] H.C. Urey, The cosmic abundances of potassium, uranium and thorium and the heat balances of the earth, the moon, and mars, Proc. Natl. Acad. Sci. USA 41 (1955) 127–144.
- [9] H. Takeda, T. Ishii, T. Arai, H. Miyamoto, Mineralogy of the Asuka 87 and 88 eucrites and crustal evolution of the HED parent body, Antarct. Met. Res. 10 (1997) 401–413.
- [10] E.J. Catanzaro, T.J. Murphy, E.L. Garner, W.R. Shields, Absolute isotopic abundance ratios and atomic weight of magnesium, J. Res. Nat. Bur. Stand. – A. Phys. Chem. 70A (1966) 453–458.
- [11] W.A. Russell, D.A. Papanastassiou, T.A. Tombrello, Ca isotope fractionation on the Earth and other solar system materials, Geochim. Cosmochim. Acta 42 (1978) 1075–1090.

- [12] T. Lee, D.A. Papanastassiou, G.J. Wasserburg, Aluminum-26 in the early solar system: fossil or fuel?, *Ap. J. Lett.* 211 (1977) L107–L110.
- [13] G.J. MacPherson, A.M. Davis, E.K. Zinner, The distribution of aluminum-26 in the early Solar System – A reappraisal, *Meteoritics* 30 (1995) 365–386.
- [14] R.W. Carlson, G.W. Lugmair, Timescales of planetesimal formation and differentiation based on extinct and extant radioisotopes, in: R.M. Canup, K. Righter (Eds.), *Origin of the Earth and Moon*, University of Arizona Press, Tucson, AZ, 2000, pp. 25–44.
- [15] T.L. Norris, A.J. Gancarz, D.J. Rokop, K.W. Thomas, Half-life of ^{26}Al , *Proc. 14th Lunar Planet. Sci. Conf.*, *J. Geophys. Res.* 88, Supplement (1983) B331–B333.
- [16] K. Nishiizumi, Preparation of ^{26}Al AMS standards, *Nuclear Instruments and Methods in Physics Research*, in: *Proc. Ninth International Symposium on Accelerator Mass Spectrometry* (2003) (preprint).
- [17] G. Srinivasan, D.A. Papanastassiou, G.J. Wasserburg, N. Bhandari, J.N. Goswami, ^{26}Al - ^{26}Mg and ^{53}Mn - ^{53}Cr systematics in the Piplia Kalan eucrite (abstract), *Lunar Planet. Sci.* XXX (1999) #1730 (CD-ROM).
- [18] G. Srinivasan, J.N. Goswami, N. Bhandari, ^{26}Al in eucrite Piplia Kalan: Plausible heat source and formation chronology, *Science* 284 (1999) 1348–1350.
- [19] J.H. Chen, G.J. Wasserburg, The isotopic composition of uranium and lead in Allende inclusions and meteorite phosphates, *Earth Planet. Lett.* 52 (1981) 1–15.
- [20] Y. Amelin, A.N. Krot, I.D. Hutcheon, A.A. Ulyanov, Lead isotopic ages of chondrules and calcium-aluminum-rich inclusions, *Science* 297 (2002) 1678–1683.
- [21] G.W. Lugmair, A. Shukolyukov, Early solar system events and timescales, *Meteorit. Planet. Sci.* 36 (2001) 1017–1026.
- [22] L. Nyquist, D. Lindstrom, D. Mittlefehldt, C.-Y. Shih, H. Wiesmann, S. Wentworth, R. Martinez, Manganese-chromium formation intervals for chondrules from the Bishunpur and Chainpur meteorites, *Meteorit. Planet. Sci.* 36 (2001) 911–938.
- [23] N.T. Kita, H. Nagahara, S. Togashi, Y. Morishita, A short duration of chondrule formation in the solar nebula: Evidence from ^{26}Al in Semarkona ferromagnesian chondrules, *Geochim. Cosmochim. Acta* 64 (2000) 3913–3922.
- [24] G. Srinivasan, A.N. Krot, A.A. Ulyanov, Aluminum-magnesium systematics in anorthite-rich chondrules and calcium-aluminum-rich inclusions from the reduced CV chondrite Efremovka, *Meteorit. Planet. Sci.* 35 (2000) A151.
- [25] J.L. Bircck, C.J. Allegre, Evidence for the presence of ^{53}Mn in the early solar system, *Geophys. Res. Lett.* 12 (1985) 745–748.
- [26] G. Srinivasan, D.A. Papanastassiou, G.J. Wasserburg, N. Bhandari, J.N. Goswami, Re-examination of ^{26}Al - ^{26}Mg systematics in the Piplia Kalan eucrite (abstract), *Lunar Planet. Sci.* XXXI (2000) #1795 (CD-ROM).
- [27] G. Srinivasan, D.A. Papanastassiou, G.J. Wasserburg, N. Bhandari, J.N. Goswami, Sm–Nd systematics and initial $^{87}\text{Sr}/^{86}\text{Sr}$ in the Piplia Kalan eucrite (abstract), *Lunar Planet. Sci.* XXX (1999) #1718 (CD-ROM).
- [28] P.C. Buchanan, D.W. Mittlefehldt, R. Hutchison, C. Koeberl, D.J. Lindstrom, M.K. Pandit, Petrology of the Indian eucrite Piplia Kalan, *Meteorit. Planet. Sci.* 35 (2000) 609–615.
- [29] D.D. Bogard, D.H. Garrison, Early thermal history of eucrites by ^{39}Ar - ^{40}Ar (abstract), *Lunar Planet. Sci.* XXXII (2001) #1138 (CD-ROM).
- [30] G. Srinivasan, ^{26}Al - ^{26}Mg systematics of A881394 eucrite (abstract), *Lunar Planet. Sci.* XXXIII (2002) #1489 (CD-ROM).
- [31] G. Srinivasan, ^{26}Al - ^{26}Mg systematics in eucrites A881394, A87122 and Vissannapeta (abstract), *Meteorit. Planet. Sci.* 37 (2002) A135.
- [32] T. LaTourette, G.J. Wasserburg, Mg diffusion in anorthite: implications for the formation of early solar system planetesimals, *Earth Planet. Sci. Lett.* 158 (1998) 91–108.
- [33] K. Roselieb, A. Jambon, Tracer diffusion of Mg, Ca, Sr, and Ba in Na-aluminosilicate melts, *Geochim. Cosmochim. Acta* 66 (2002) 109–123.
- [34] D.N. Schramm, F. Tera, G.J. Wasserburg, The isotopic abundance of ^{26}Mg and limits on ^{26}Al in the early solar system, *Earth Planet. Sci. Lett.* 10 (1970) 44–59.
- [35] P.W. Warren, Magnesium oxide-iron oxide mass balance constraints and a more detailed model for the relationship between eucrites and diogenites, *Meteorit. Planet. Sci.* 32 (1997) 945–963.
- [36] A. Ghosh, H.Y. McSween, A thermal model for the differentiation of Asteroid 4 Vesta, based on radiogenic heating, *Icarus* 134 (1998) 187–206.
- [37] H.S. Carslaw, J.C. Jaeger, *Conduction of Heat in Solids*, 2nd edn., Clarendon Press, Oxford, 1959, 519 pp.
- [38] R. Greenberg, J.F. Wacker, W.K. Hartmann, C.R. Chapman, *Planetesimals to planets: Numerical simulations of collisional evolution*, *Icarus* 35 (1978) 1–26.
- [39] Y. Nakagawa, C. Hayashi, K. Nakazawa, Accumulation of planetesimals in the solar nebula, *Icarus* 54 (1983) 361–376.
- [40] G. Wetherill, Origin of the asteroid belt, in: R.P. Binzel, T. Gehrels, M.S. Matthews (Eds.), *Asteroids II*, University of Arizona Press, Tucson, AZ, 1989, pp. 661–680.
- [41] M.J. Gaffey, J.F. Bell, D.P. Cruikshank, Reflectance spectroscopy and asteroid surface mineralogy, in: R.P. Binzel, T. Gehrels, M.S. Matthews (Eds.), *Asteroids II*, University of Arizona Press, Tucson, AZ, 1989, pp. 98–127.
- [42] R.E. Grimm, H.Y. McSween, Heliocentric zoning of the asteroid belt by aluminum-26 heating, *Science* 259 (1993) 653–655.
- [43] H. Takeda, Mineralogical records of early planetary processes on the howardite, eucrite, diogenite parent body with reference to Vesta, *Meteorit. Planet. Sci.* 32 (1997) 841–853.
- [44] P.H. Warren, Differentiation of siderophile elements in the Moon and the HED parent asteroid, *Antarctic Meteorites XXIV*, 1999, pp. 185–186.

- [45] Y. Ikeda, H. Takeda, A model for the origin of basaltic achondrites based on the Yamato 7308 howardite, Proc. 15th Lunar Planet. Sci. Conf., J. Geophys. Res. 90, Supplement (1985) C649–C663.
- [46] K. Saiki, H. Takeda, T. Ishii, Mineralogy of Yamato-791192, HED breccia and relationship between cumulate eucrites and ordinary eucrites, *Antarct. Meteor. Res.* 14 (2001) 28–46.
- [47] A. Yamaguchi, T. Sekine, H. Mori, Shock experiments on a preheated basaltic eucrite, *Shock Chemistry and Meteoritic Applications*, Springer-Verlag, 2002, in press.
- [48] H. Takeda, D.D. Bogard, D.W. Mittlefehldt, D.H. Garrison, Mineralogy, petrology, chemistry, and ^{39}Ar – ^{40}Ar and exposure ages of the Caddo County IAB iron: Evidence for early partial melt segregation of a gabbro area rich in plagioclase-diopside, *Geochim. Cosmochim. Acta* 64 (2000) 1311–1327.
- [49] A. Yamaguchi, G.J. Taylor, K. Keil, C. Floss, G. Crozaz, L.E. Nyquist, D.D. Bogard, D.H. Garrison, Y.D. Reese, H. Wiesmann, C.-Y. Shih, Post-crystallization reheating and partial melting of eucrite EET90020 by impact into the hot crust of asteroid 4 Vesta, *Geochim. Cosmochim. Acta* 65 (2001) 3577–3599.
- [50] A. Yamaguchi, G.J. Taylor, K. Keil, Metamorphic history of the eucritic crust of 4 Vesta, *J. Geophys. Res.* 102 (1997) 13381–13386.
- [51] A. Ghosh, S.J. Weidenschilling, H.Y. McSween Jr., F. Nimmo, Accretion and its effect on the thermal history of Mars, *Lunar Planet. Sci. XXXIII #1885* (2002) (CD-ROM).
- [52] J.F. Bell, D.R. Davis, W.K. Hartmann, M.J. Gaffey, Asteroids: The big picture, in: R.P. Binzel, T. Gehrels, M.S. Matthews (Eds.), *Asteroids II*, University of Arizona Press, Tucson, AZ, 1989, pp. 921–945.